

Supporting Information

Carbonylation of Dimethyl Ether to Methyl Acetate over SSZ-13

Marcella Lusardi,[†] Thomas T. Chen,[‡] Matthew Kale,^{†,‡} Jong Hun Kang,[†] Matt Neurock,[‡] Mark E. Davis^{†,*}

[†]Chemical Engineering, California Institute of Technology, Pasadena, CA 91125 United States

[‡]Chemical Engineering and Materials Science, University of Minnesota, Minneapolis, MN 55455 United States

**Corresponding Author:* mdavis@cheme.caltech.edu

DFT computational methods:

Harmonic frequency calculations, partial Hessian vibration analysis (PHVA), were performed to determine the zero-point vibrational energies (ZPVE), vibrational enthalpies (H_{vib}), and vibrational free energies (G_{vib}) required to calculate the enthalpies, entropies, and free energies of reactants, products, and transition state structures. The PHVA were performed with SCF convergence of 10^{-8} eV using the central difference method with atom displacement of 0.015 Å. The mobile adsorbate method is applied in determination of adsorption free energies and considered appropriate due to the loose adsorptive binding of CO ($\Delta H_{\text{ads}} \sim -30$ kJ mol⁻¹) to the methoxide sites in CHA. The mobile adsorbate method has been shown to be appropriate for zeolite systems with adequate prediction of alkane and alkene physisorption entropies in zeolites, within 10 - 15 J mol⁻¹ K⁻¹.¹ The n rotational and translational degrees of freedom are considered mobile if their harmonic frequencies are < 100 cm⁻¹ and if the normal modes show little coupling with internal zeolite vibrations. From this analysis, CO, DME, and MA are determined to have 3D free translation and 3D free rotation in SSZ-13 in which case the diameter of the 8MR windows (3.72 Å) will be used in the free translation partition function. The translational and rotational frequencies are selected and replaced with their respective partition function. This is done by decoupling both translation and rotation through application of an Eckart condition projection matrix to the Hessian. This procedure is described in *A Practical Introduction to the Simulation of Molecular Systems*.² The CO addition transition state and resultant acylium ion are assumed to be immobile adsorbates due to a necessity in being tightly adsorbed near the acid site.

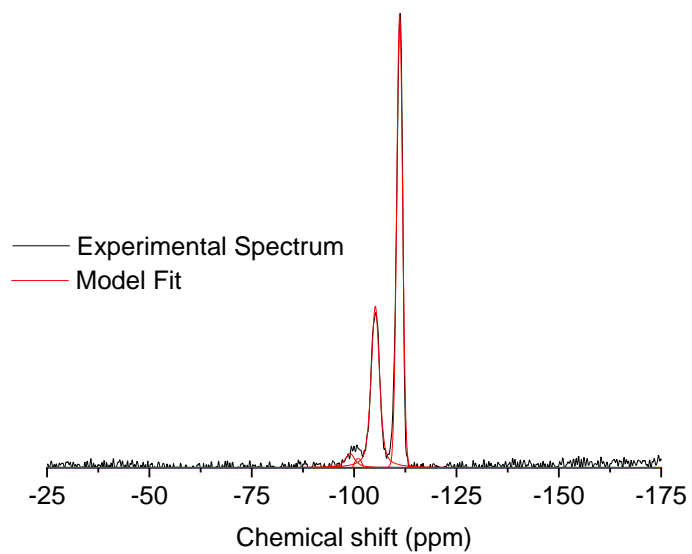


Figure S1. Experimental ^{29}Si MAS NMR spectrum for SSZ-13 (9) in the NH_4^+ -form plotted with the spectrum model fit (DMFit).

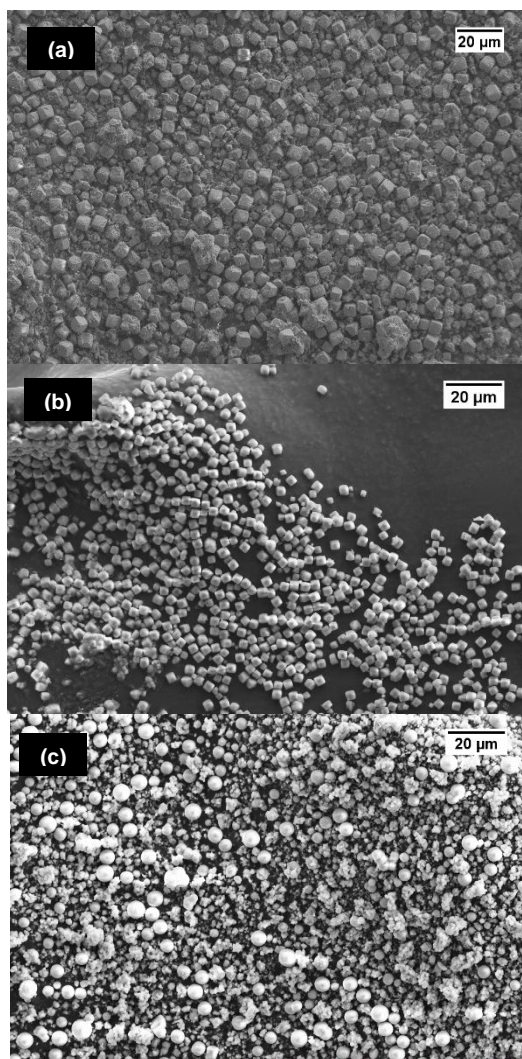


Figure S2. SEM images of (a) SSZ-13 (30), (b) SSZ-13 (22), and (c) SSZ-13 (9) in the NH_4^+ -form.

Table S1. Particle diameters measured in SEM images

Sample	Particle diameters (μm)
SSZ-13 (9)	3.6 +/- 1.3
SSZ-13 (22)	3.1 +/- 0.2
SSZ-13 (30)	3.9 +/- 1.2

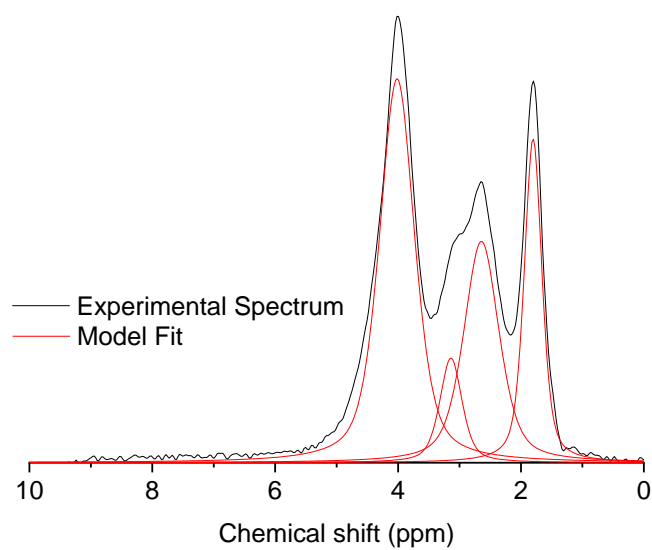


Figure S3. Experimental ^1H MAS NMR spectrum on the dehydrated SSZ-13 (9) in the H^+ -form plotted with the spectrum model fit (DMFit).

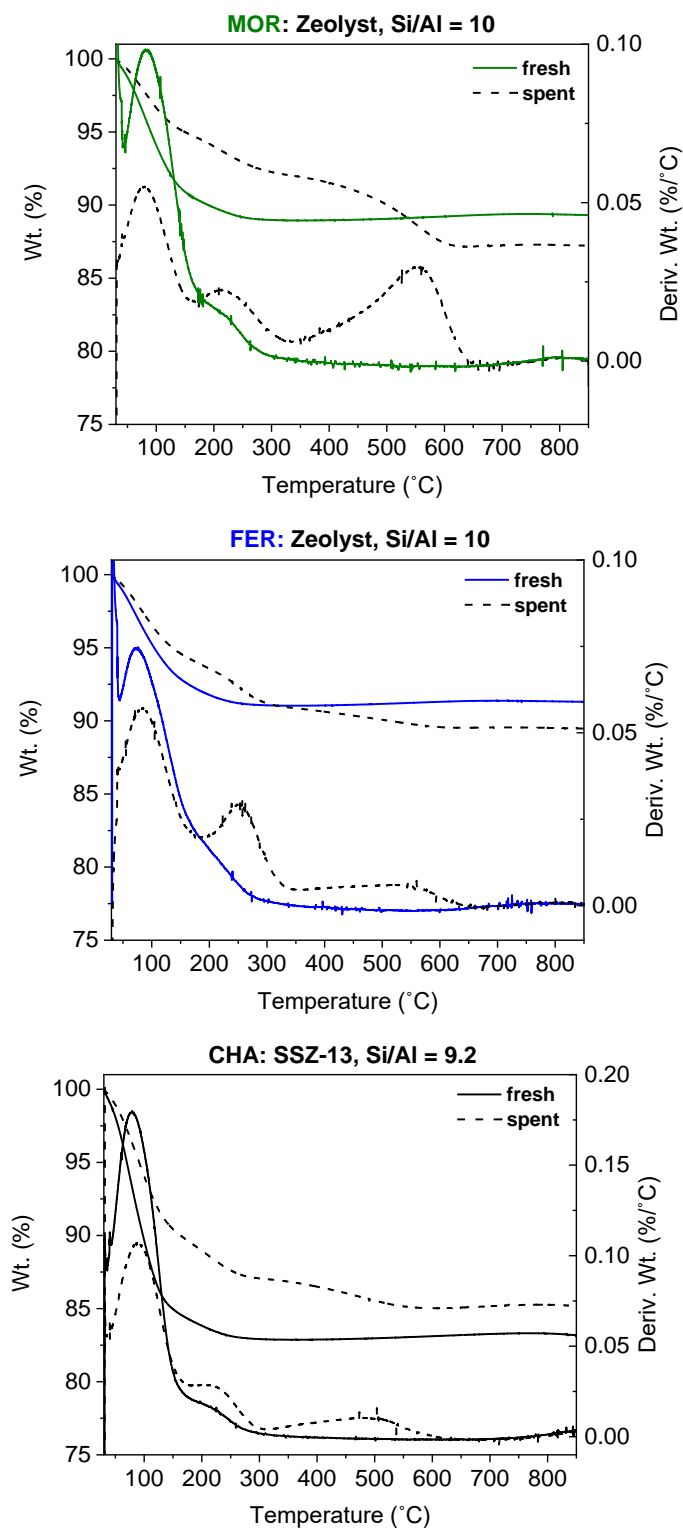


Figure S4. TGA profiles of fresh (solid line) catalysts and spent (dashed line; 24 hr on stream) catalysts. (20 sccm air, 10 °C min⁻¹ ramp).

Table S2. Carbon deposition amount on each spent catalyst after 24 hr on stream calculated from TGA profiles and approximated molecular formula for coke

Coke formula: CH		
Framework	Wt.% loss: 300 to 650 °C	Mole carbon _{coke} (μmol)
MOR	5.51%	635
FER	1.83%	210
CHA	2.29%	264

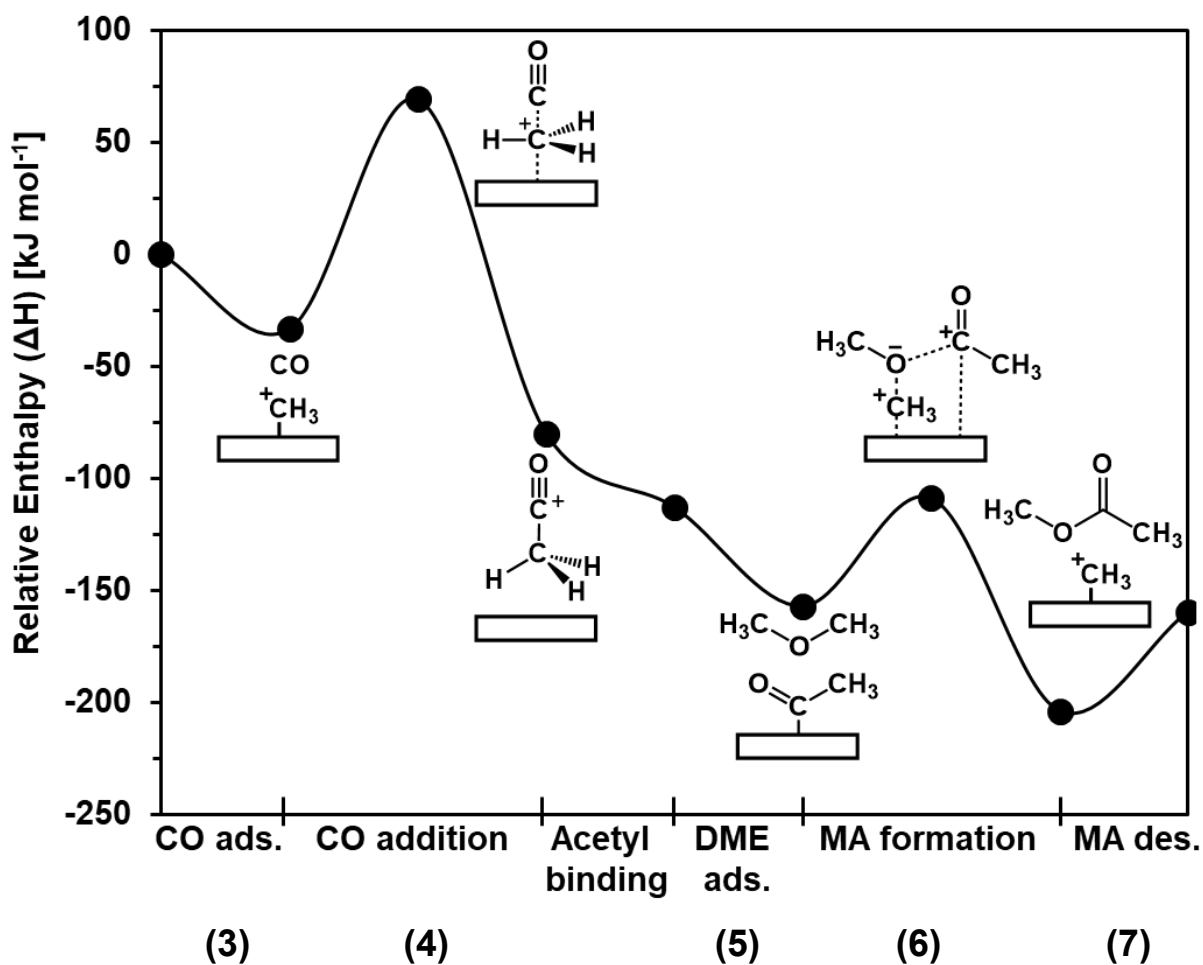


Figure S5. Enthalpy pathway for the full catalytic turnover for the carbonylation of DME to MA assuming a surface saturated with methoxy groups.

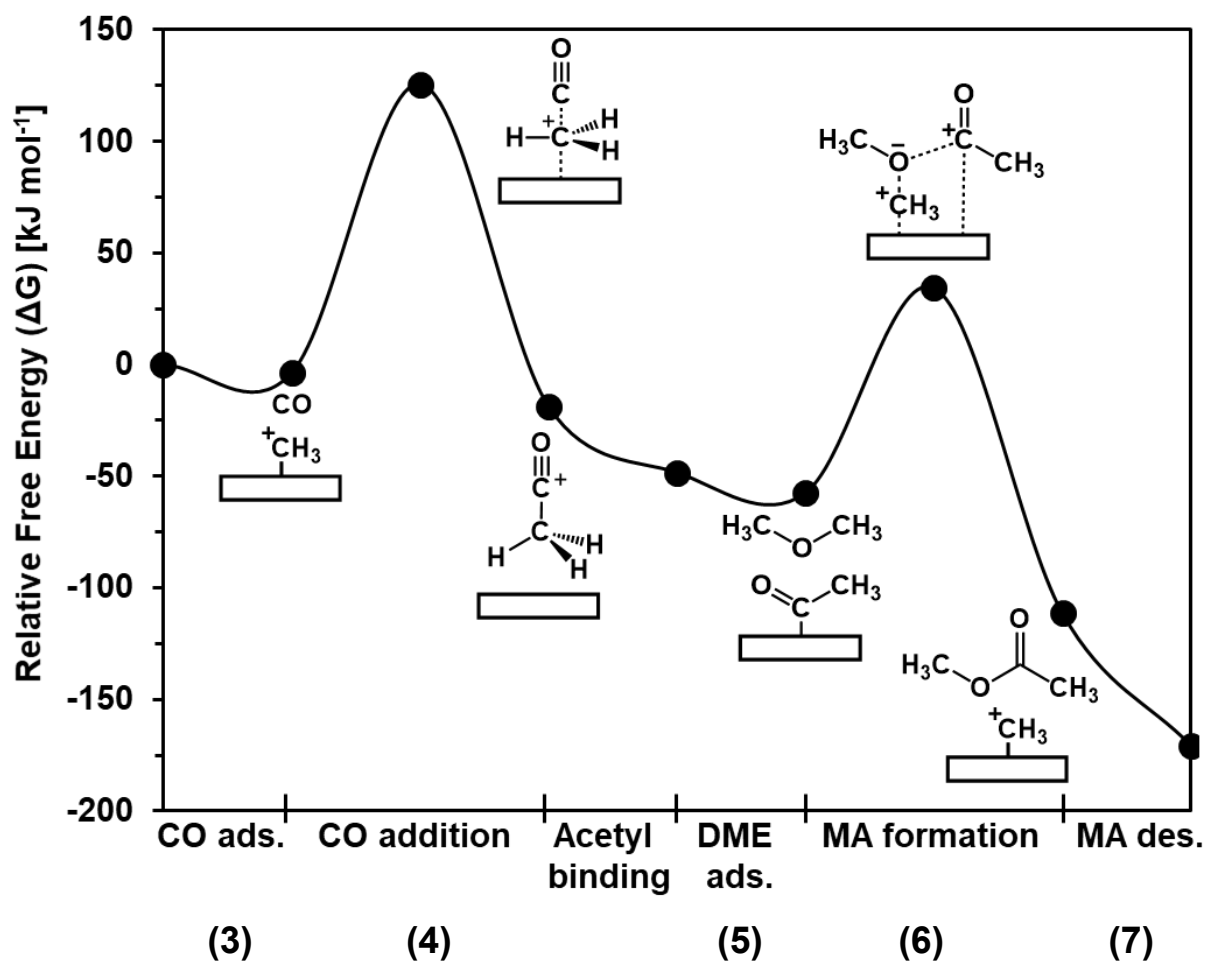


Figure S6. Free energy pathway for the full catalytic turnover for the carbonylation of DME to MA assuming a surface saturated with methoxy groups.

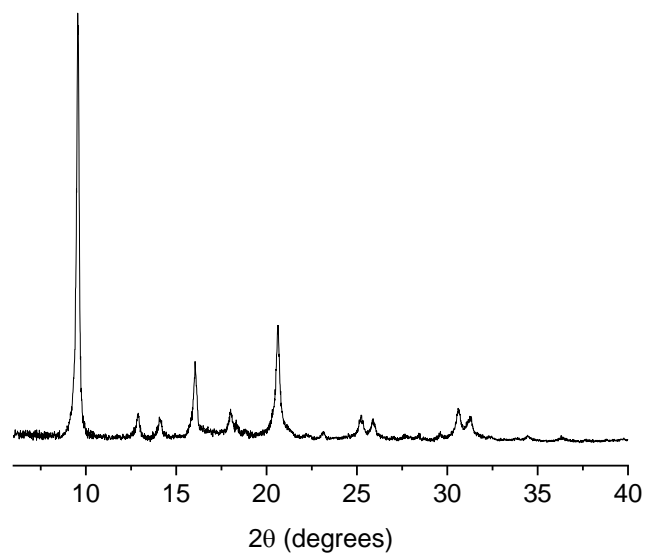


Figure S7. XRD pattern for as-synthesized SAPO-34.

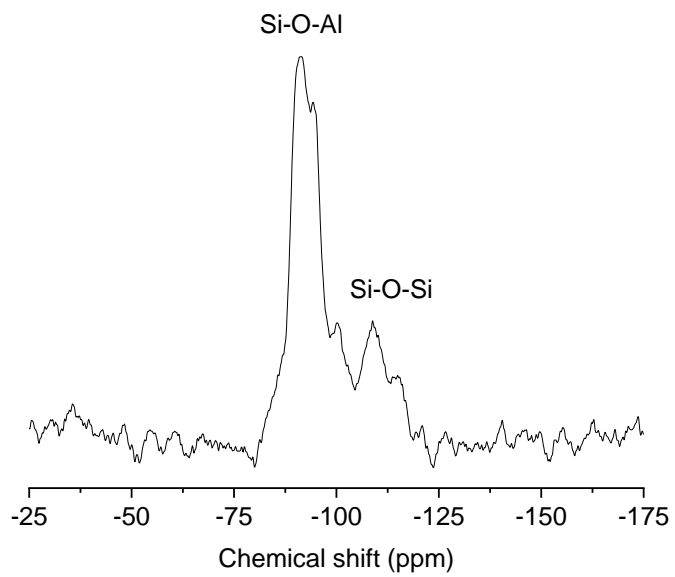


Figure S8. ^{29}Si MAS NMR on calcined (H^+ -form) SAPO-34.

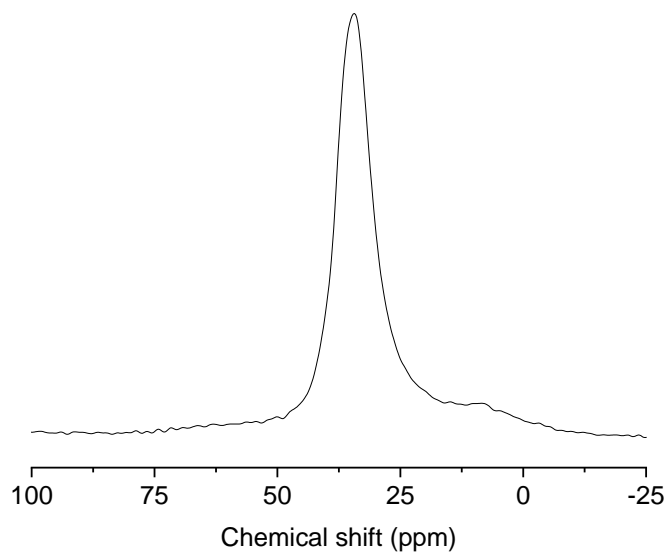


Figure S9. ^{27}Al MAS NMR on calcined (H^+ -form) and dehydrated SAPO-34.

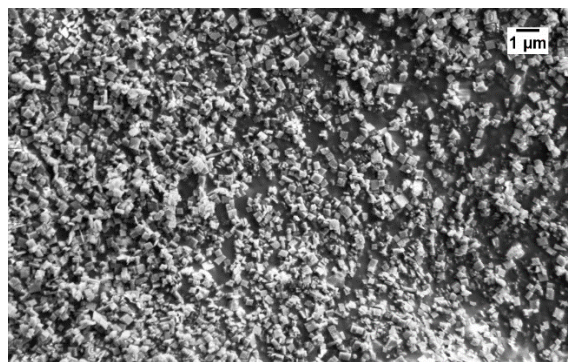


Figure S10. SEM image of calcined (H^+ -form) SAPO-34. SEM-EDS analysis measured 9 ± 1 at.% Si in the SAPO sample.

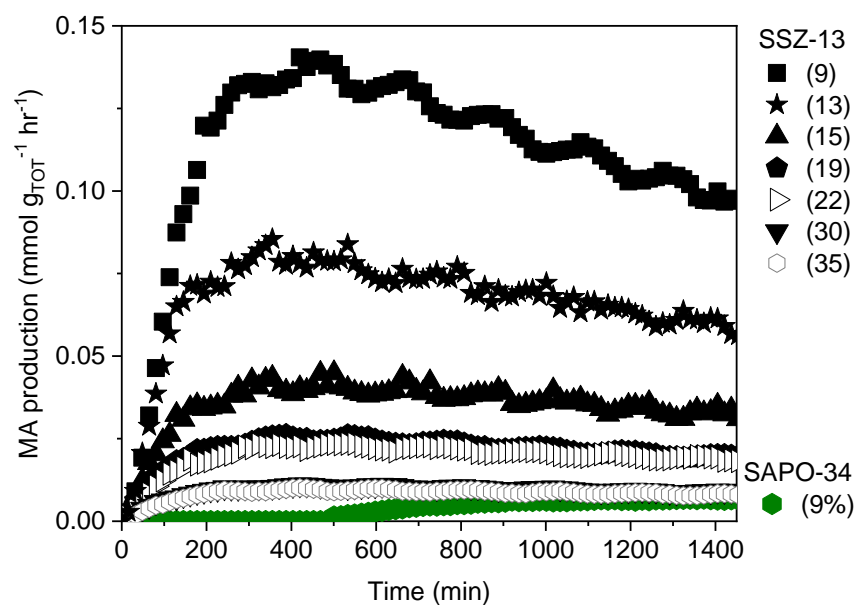


Figure S11. MA production rates over time for the SSZ-13s compared to the SAPO-34 sample (9 at% Si).

Table S3. Comparison of intrinsic activation barriers for CO addition to CH_3^+ in SSZ-13 versus SAPO-34 at different O sites ($T = 165^\circ\text{C}$)

O Site	Cationic position	SSZ-13	SAPO-34
		ΔH_A (kJ mol ⁻¹)	ΔH_A (kJ mol ⁻¹)
O1	SIII'	101.5	111.8
O2	SIII'	102.6	111.2
O3	SII	114.0	121.8
O4	—	112.0	127.0

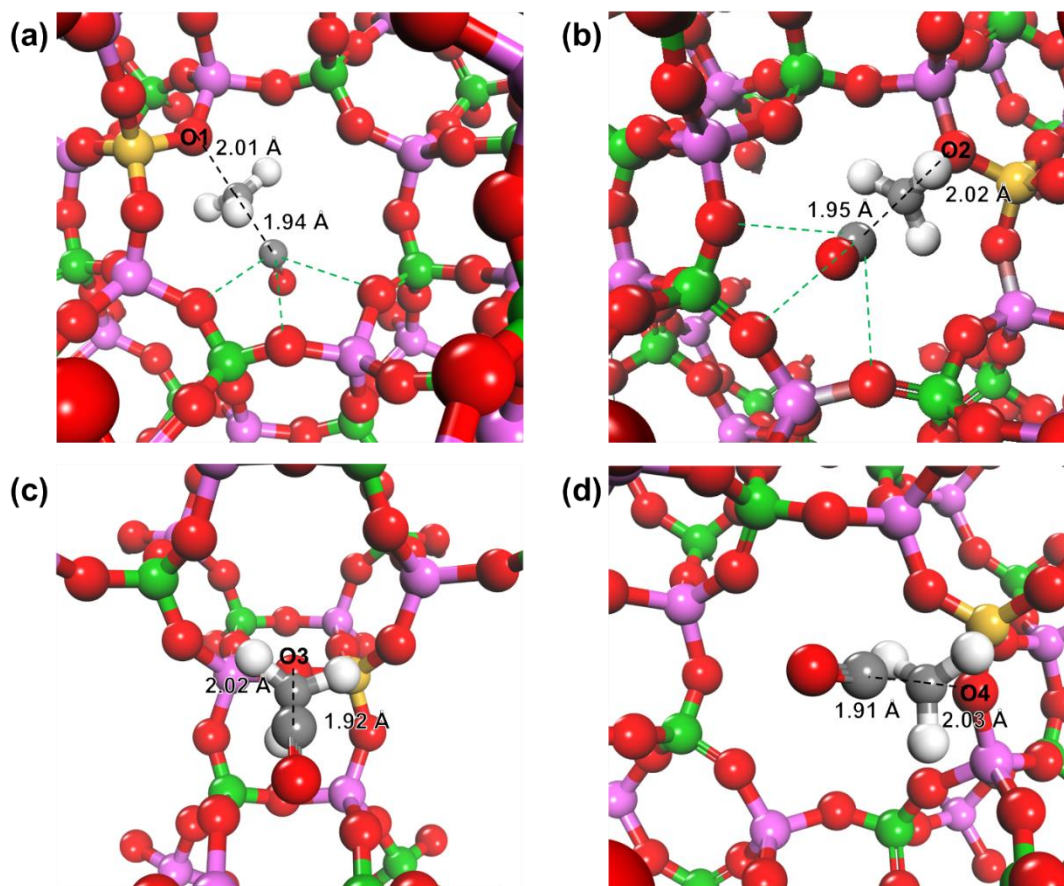


Figure S12. Transition state for CO addition to CH_3^+ originating from the four O sites in SAPO-34: (a) O1 site, (b) O2 site, (c) O3 site, and (d) O4 site. The dotted green lines indicate close contact interactions ($< 3.50 \text{ \AA}$) between the $(\text{C})\equiv\text{O}$ of the transition state and O of the SAPO-34 framework. $\text{HC}_3\text{-O}_{\text{zeolite}}$ and the $\text{HC}_3\text{-O}_{\text{zeolite}}$ bond distances for transition states in SSZ-13 and SAPO-34 are nearly invariant, which is expected given their shared pore topology. Atom colors: P (green), Al (purple), Si (yellow), O (red), C (grey), and H (white).

References

- (1) De Moor, B. A.; Ghysels, A.; Reyniers, M.-F.; Van Speybroeck, V.; Waroquier, M.; Marin, G. B. Normal Mode Analysis in Zeolites: Toward an Efficient Calculation of Adsorption Entropies. *J. Chem. Theory Comput.* **2011**, 7, 1090–1101.
- (2) Field, M. J. *A Practical Introduction to the Simulation of Molecular Systems*, 2nd ed.; Cambridge University Press: Cambridge, 2007.